High-Intensity Illuminated Annealing of Industrial SHJ Solar Cells: A Pilot Study

Matthew Wright, Anastasia Soeriyadi, Brendan Wright, Dmitry Andronikov, Ilia Nyapshaev, Sergey Abolmasov, Alexey Abramov, and Brett Hallam

***Abstract*—Here, we demonstrate the effectiveness of illuminated annealing using high-intensity light to improve the efficiency of industrial n-type silicon heterojunction (SHJ) solar cells. The application of high intensity laser light during annealing at 200 °C led to efficiency improvements as large as 0.7 $\%_{\mathrm{abs}}$ and final efficiencies as high as 24.5%. This was demonstrated on industrial SHJ solar cells from five different manufacturers, indicating the robust application of this technique. We show that the annealing process with high-intensity light leads to significant efficiency enhancements compared to previous observations using light soaking under 1-sun conditions, meaning the process can be completed in 30 s, rather than hours. The observed enhancements were related to increased V_{OC} and fill factor. If this approach can be tailored to time scales amenable with mass production, the associated efficiency enhancements could drive reductions in the levelized cost of electricity for SHJ solar cells, making them more competitive in the face of existing technologies.**

***Index Terms*—Illuminated annealing, light soaking, silicon heterojunction (SHJ), surface passivation.**

I. Introduction

THE current world record efficiency of 26.7% for a single junction silicon solar cell was achieved using silicon heterojunction (SHJ) device architecture [1]. The SHJ cell architecture allows for very high open-circuit voltages (V_{OC}), of up to 750 mV [2]. The ability to achieve such high V_{OC} is related to the excellent surface passivation provided by the intrinsic hydrogenated amorphous silicon (a-Si:H) layers, which significantly reduce recombination at the surfaces [3]–[5]. Additionally, the carrier selectivity of the contacts is determined by thin, doped amorphous silicon layers, which removes the need for a thermally diffused homojunction. The lack of a heavily doped surface region reduces Auger recombination, increasing the achievable V_{OC}. Another advantage of SHJ cells is the lower temperature coefficient, meaning that modules perform better when operating under elevated temperatures in the field [6]. Due to these advantages, SHJ cells are very suitable as the bottom cell in perovskite/silicon tandem solar cells [7]–[9]. The design of the SHJ structure, which relies on intrinsic and doped a-Si:H layers, changes the processing temperature requirements compared to other cell designs, such as passivated emitter and rear cell (PERC) and tunneling oxide passivating contact (TOPCon) cells [10]–[14]. Both PERC and TOPCon solar cells include a thermal diffusion and contact firing process, which occur at temperatures $>$700 °C. However, during SHJ processing, the temperature is kept below $\sim$200 °C [4]. Special low temperature silver paste is used for contact formation at this low temperature [15]. The main reason for the temperature constraint is the instability of the surface passivation from the a-Si:H layers. At elevated temperature, the chemical passivation of surface states begins to deteriorate, due to the rupturing of Si-H bonds at the interface [16]–[18].

Extensive studies have shown instabilities in p-type solar cells under the presence of light and elevated temperature. Efficiency reduction in p-type solar cells are related to two primary forms of defects: first, boron-oxygen light induced degradation [19]–[21]; and second, light and elevated temperature induced degradation (LeTID) [22]–[24]. Multiple reports have displayed efficiency enhancements in n-type SHJ cells using light soaking [25], [26]. In 2016, Kobayashi *et al.* [27] reported on changes in the efficiency of n-type SHJ solar cells under extensive light soaking with an illumination intensity of 1-sun. Remarkably, they showed that the efficiency of SHJ solar cells increased following light soaking by up to 0.3 $\%_{\mathrm{abs}}$. This increase was related to improved V_{OC} and fill factor (FF), which was attributed to a reduction in interfacial defect states [27], [28]. They also showed similar kinetics of increased efficiency following current injection, indicating that the increase is related to the generation of carriers in the c-Si layer. A follow-up publication showed a similar result on minimodules with n-type SHJ cells [29]. The time frame to reach the saturated efficiency gain of 0.3 $\%_{\mathrm{abs}}$ was $\sim$15 h. This is far too long to be incorporated into a production scenario. Multiple reports have shown that the use of high-intensity light produced by a laser can significantly accelerate the rate of degradation in p-type PERC solar cells

Manuscript received July 18, 2021; revised September 30, 2021; accepted October 11, 2021. Date of publication December 10, 2021; date of current version December 23, 2021. This work was supported in part by the Australian Centre for Advanced Photovoltaics (ACAP) and in part by the Australian Renewable Energy Agency (ARENA) under Grant 2017/RND005. *(Matthew Wright and Anastasia Soeriyadi contributed equally to this work.) (Corresponding author: Matthew Wright.)*

Matthew Wright, Anastasia Soeriyadi, Brendan Wright, and Brett Hallam are with the School of Photovoltaic and Renewable Energy Engineering, University of New South Wales, Sydney, NSW 2052, Australia (e-mail: matthew.wright@materials.ox.ac.uk; anastasia.soeriyadi@unsw.edu.au; brendan.wright@unsw.edu.au; brett.hallam@unsw.edu.au).

Dmitry Andronikov, Ilia Nyapshaev, Sergey Abolmasov, and Alexey Abramov are with the R&D Center TFTE LLC, St. Petersburg 194064, Russia, and also with the Ioffe Institute, Russian Academy of Sciences, St-Petersburg 194064, Russia (e-mail: d.andronikov@hevelsolar.com; i.nyapshaev@hevelsolar.com; s.abolmasov@hevelsolar.com; a.abramov@hevelsolar.com).

Color versions of one or more figures in this article are available at https://doi.org/10.1109/JPHOTOV.2021.3122932.

Digital Object Identifier 10.1109/JPHOTOV.2021.3122932

TABLE I
AVERAGE PHOTOVOLTAIC CHARACTERISTICS OF INDUSTRIAL SHJ CELLS FROM HEVEL LLC

Group		J_{SC} (mA/cm^2)	V_{OC} (mV)	FF (%)	R_S (Ω·cm^2)	Efficiency (%)
1	As Received	37.70 ± 0.11	735.9 ± 1.3	81.2 ± 0.4	1.10 ± 0.04	22.53 ± 0.12
	Processed	37.74 ± 0.12	741.0 ± 1.1	82.6 ± 0.3	0.97 ± 0.14	23.11 ± 0.11
	Change	+0.04	+5.1	+1.4	-0.13	+0.58
2	As Received	37.67 ± 0.09	729.4 ± 2.3	77.3 ± 0.5	1.92 ± 0.11	21.25 ± 0.09
	Processed	37.73 ± 0.09	735.9 ± 1.6	78.8 ± 0.3	1.59 ± 0.07	21.88 ± 0.08
	Change	+0.06	+6.5	+1.5	-0.33	+0.63

[30], [31]. It would be advantageous if these approaches could be used to accelerate the observed efficiency enhancements in n-type SHJ solar cells so that the time frame of the process could be reduced.

In this work, we show enhancements in SHJ solar cells under light soaking with high-intensity light from a laser. Efficiency enhancements of up to $0.7\%_{\mathrm{abs}}$ were observed, which is larger than the enhancements previously reported under 1-sun conditions. Importantly, we demonstrate that this approach works for industrial cells from five different manufacturers. The use of high-intensity light significantly accelerates the performance enhancement, with a processing time-scale on the order of seconds rather than hours. This short time-scale means that temperatures exceeding 200 °C can be explored, which contradicts conventional thinking on the potential temperature processing windows for SHJ solar cells. We also observe that illuminated annealing leads to reduced short-circuit current density (J_{SC}) for cells from one manufacturer. This indicates that the enhancement is sensitive to the processing conditions used.

II. EXPERIMENTAL DETAILS

The primary pilot study experiment in this work was performed on n-type SHJ solar cells, fabricated in an industrial environment by Hevel LLC. The SHJ cells were all M2, busbarless and bifacial. Two distinct groups of cells were studied; results from 50 cells in each group are described in this article. The difference in the groups is the cell efficiency, group 1 had a starting efficiency of 22.53 ± 0.12%, and group 2 had a starting efficiency of 21.25 ± 0.09%. Groups with two significantly different efficiency bins were used deliberately to compare the effect of the illuminated annealing depending on the initial cell efficiency. In addition to the 100 cells from Hevel LLC, the demonstration of illuminated annealing in this report was performed on n-type industrial SHJ solar cells from a range of leading manufacturers. Due to commercial sensitivity, the exact processing methods and company names are not disclosed for each set of cells. The cells were heated on a hot plate with a setpoint temperature of 200 °C and were illuminated with a continuous wave ($\lambda = 980$ nm) solid state diode laser with monochromatic illumination intensity of ∼55 kW/m^2. Accounting for photon density, this is equivalent to approximately 100 suns. This illumination intensity caused the sample temperature to increase to ∼255 °C during exposure. The time of the process used was 30 s. This post-cell illuminated annealing was performed at The University of New South Wales (UNSW). Current-voltage (*I–V*) measurements were performed in house at Hevel LLC under standard testing conditions. The *I–V* measurements before and after the illuminated annealing for cells from all other companies were performed at UNSW under standard testing conditions using either a Wavelabs Sinus 220 or pvtools Loana *I–V* testing system. Photoluminescence (PL) images were obtained using a BT imaging LIS-R3 luminescence imaging tool before and after the post-cell process [32]. The same tool was used to generate the series resistance mapping, based on a methodology developed by Kampwerth *et al.* [33].

III. RESULTS AND DISCUSSION

First, high intensity illuminated annealing using a laser was performed at UNSW on 100 n-type SHJ cells fabricated in an industrial environment at Hevel LLC. Table I shows the average *I–V* parameters before and after the process for each group, as well as the absolute change in each parameter caused by the processing. Fig. 1 graphically displays the change in J_{SC}, V_{OC}, FF, and efficiency using box plots. Fig. 1 displays a clear increase in efficiency after the illuminated annealing. The average efficiency improves by $0.58\%_{\mathrm{abs}}$ ($2.58\%_{\mathrm{rel}}$) and $0.63\%_{\mathrm{abs}}$ ($2.96\%_{\mathrm{rel}}$) for group 1 and group 2, respectively. It appears these improvements are slightly more pronounced when the starting efficiency is lower. However, significant improvements are still observed on group 1, with initial efficiencies exceeding 22.5%. This efficiency increase under high intensity illumination conditions, which occurs during the 30 s process, is much larger than that observed previously under 1-sun illumination [27]. No statistically significant changes were observed in the J_{SC}, the increased efficiency is related to changes in both V_{OC} and FF. The increased FF can be correlated with a reduction in series resistance (R_S). The R_S reduced by 0.13 Ω·cm^2 (11.8%) and 0.33 Ω·cm^2 (16.9%) for group 1 and group 2, respectively.

This observed efficiency enhancement is promising, particularly considering that these results are achieved using cells fully fabricated in an industrial environment and with a relatively large sample size of 100 cells. The fabrication of industrial n-type SHJ cells is a rapidly evolving landscape. Aspects of cell design, such as the metallization scheme and structure/approach for the n-doped layer, as well as the deposition tools used, are constantly updating. This is leading to impressive annual increases in the average production cell efficiencies [34]. To provide further validation for the observations in Fig. 1, the same high intensity illuminated annealing process was applied to n-type SHJ cells from a range of different leading cell manufacturers. All cells were treated at a sample temperature of ∼255 °C under 55 kW/m^2 laser illumination intensity. Fig. 2 displays a summary of the changes in efficiency for cells that have been subjected to

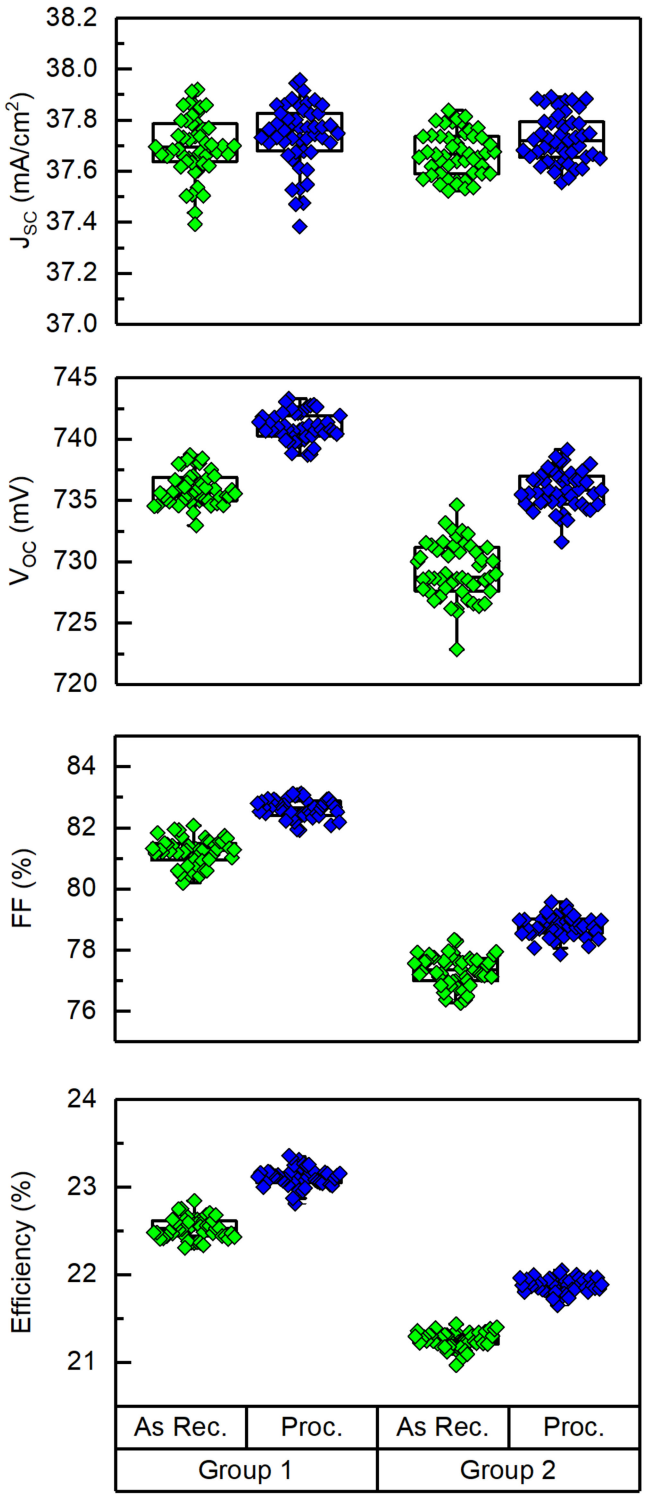

Fig. 1. Comparison of J_{SC}, V_{OC}, FF, and efficiency for both as-received (As Rec.) and processed (Proc.) cells.

illuminated annealing for 30 s. All cells used commercial n-type Cz wafers and were fabricated in a fully industrial environment.

The sample size of the experiment varied from 9 to 50. The results from the Hevel group 1 cells are also shown in Fig. 2. This presents a positive view of the impact of high-intensity illuminated annealing on industrial n-type SHJ cells. For five of the six companies displayed, efficiency enhancement ranges from $0.37\%_{\mathrm{abs}}$ to $0.70\%_{\mathrm{abs}}$. However, for one company, the efficiency enhancement was only $0.06\%_{\mathrm{abs}}$. The presented results show significant efficiency enhancements on cells with a very wide range of starting efficiency, from 21.67% to >24.00%. Five of the six companies show a larger efficiency gain under these high intensity illumination conditions compared with the light soaking under 1-sun conditions reported by Kobayashi *et al.* [27]. This highlights the potential of using high intensity light to improve the efficiency of n-type SHJ cells. In all cases except for Company Y, the J_{SC} is remarkably stable before/after the high intensity illuminated annealing. For Company Y, the J_{SC} reduces by $\sim$0.3 mA/cm^2, indicating that the response of these cells is different. This is discussed further below. The improvements in efficiency are attributed to increases in V_{OC} and FF. To investigate the spatial distribution of these changes PL imaging and R_S mapping was used.

Fig. 3(a) displays open-circuit PL images before and after the high intensity illuminated annealing on n-type SHJ cells from company X, measured under 1-sun illumination conditions. A clear increase in the PL counts can be observed, depicted graphically in the histogram (right). The peak shifts towards higher counts, with a tighter distribution. The cell is impacted by processing marks. It appears the illuminated anneal improves the lifetime in these dark regions caused by processing marks, as well as generally in unaffected areas of the cell. The defectivity caused by processing marks can also have an impact on the FF [35]. To study spatial variations in FF, R_S mapping of the same cell was also taken before/after illuminated annealing. These are displayed in Fig. 3(b). This shows two distinct benefits of the illuminated annealing: first, a reduction in the mean R_S value; and second, a reduction in standard deviation of the spatially measured R_S. This change in the distribution is clearly depicted in the accompanying histogram. The R_S can be very sensitive to the thin layers in the contact stack. Busbar to busbar resistance measurements (not shown) indicated that the illuminated annealing was not causing a reduction in the resistance in the metal. Thus, we tentatively ascribe the reduced R_S to improved conduction in the contact stack (a-Si:H(i)/a-Si:H(doped)/ITO). The broader distribution on the as-received sample may indicate that the R_S is sensitive to spatial nonuniformities in these layers. The tighter spread in the values following illuminated annealing may indicate that the annealing causes the FF to be less sensitive to spatial nonuniformities in the deposited layers. The corresponding R_S value extracted from the *I–V* curve reduced from 1.12 ± 0.17 to 0.83 ± 0.13 Ω·cm^2. The result in Fig. 3(b) indicates that the reduction in R_S has a large impact on the FF improvement. In order to help quantify this, the FF, pseudo fill factor (pFF) and R_S for cells from Company X are plotted in Fig. 4. As shown, the FF increased from $77.90 \pm 0.82\%$ to $79.90 \pm 0.76\%$ after the high intensity illuminated anneal. Correspondingly, pFF increased from $83.53 \pm 0.29\%$ to $83.95 \pm 0.33\%$. Therefore, the absolute change in FF and pFF was $2.00\%_{\mathrm{abs}}$ and $0.42\%_{\mathrm{abs}}$, respectively. The pFF provides a measure of FF without the impact of resistive losses. So, $0.42\%_{\mathrm{abs}}$ of the changes (approximately 20% of the total change in FF) are not related to changes in resistance. Therefore, the

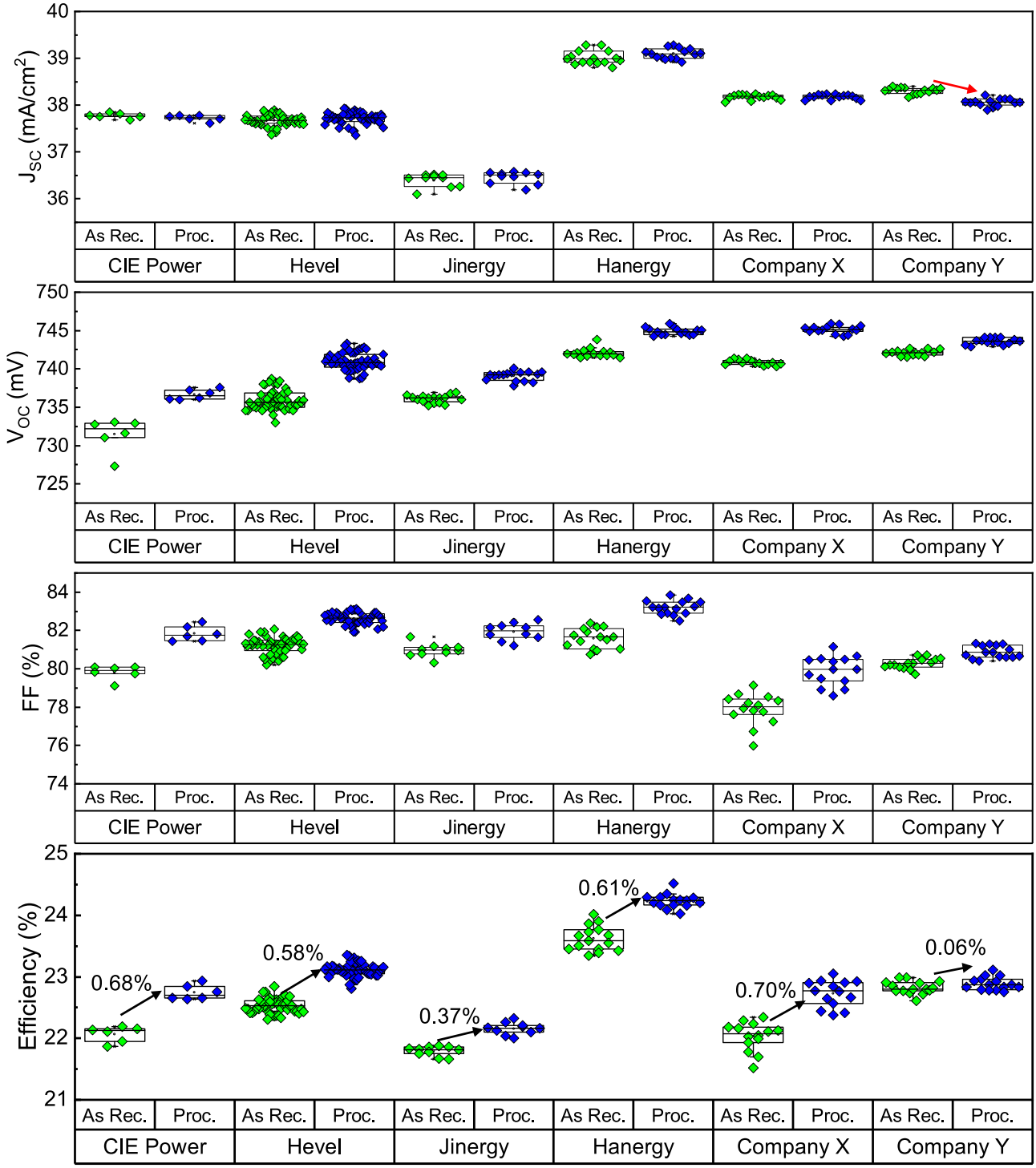

Fig. 2. Box plots showing the impact of illuminated annealing on the efficiency of industrial n-type SHJ solar cells sourced from five different companies. The company name is displayed on the *x* axis, in one case; the company named is withheld from publication.

remaining 1.58%$_{\mathrm{abs}}$ increase can be attributed to the reduced R_S. This represents approximately 80% of the 2.00%$_{\mathrm{abs}}$ FF improvement, indicating that R_S dominates the modulation of FF.

Multiple reports have shown that the changes in passivation at the a-Si:H/c-Si interface via annealing is related to a change in the density of interfacial states via hydrogen passivation, rather than a modulation of fixed charge at the interface [36], [37]. Specifically, this hydrogen passivation is facilitated by a transition from a higher hydride state in the a-Si:H film, to a monohydride c-Si surface state [16]. Mahtani *et al.* [28] showed that modulating the metastability of the a-Si:H layers via light soaking can lead to improvements in effective lifetime, which was particularly pronounced for surface passivation containing

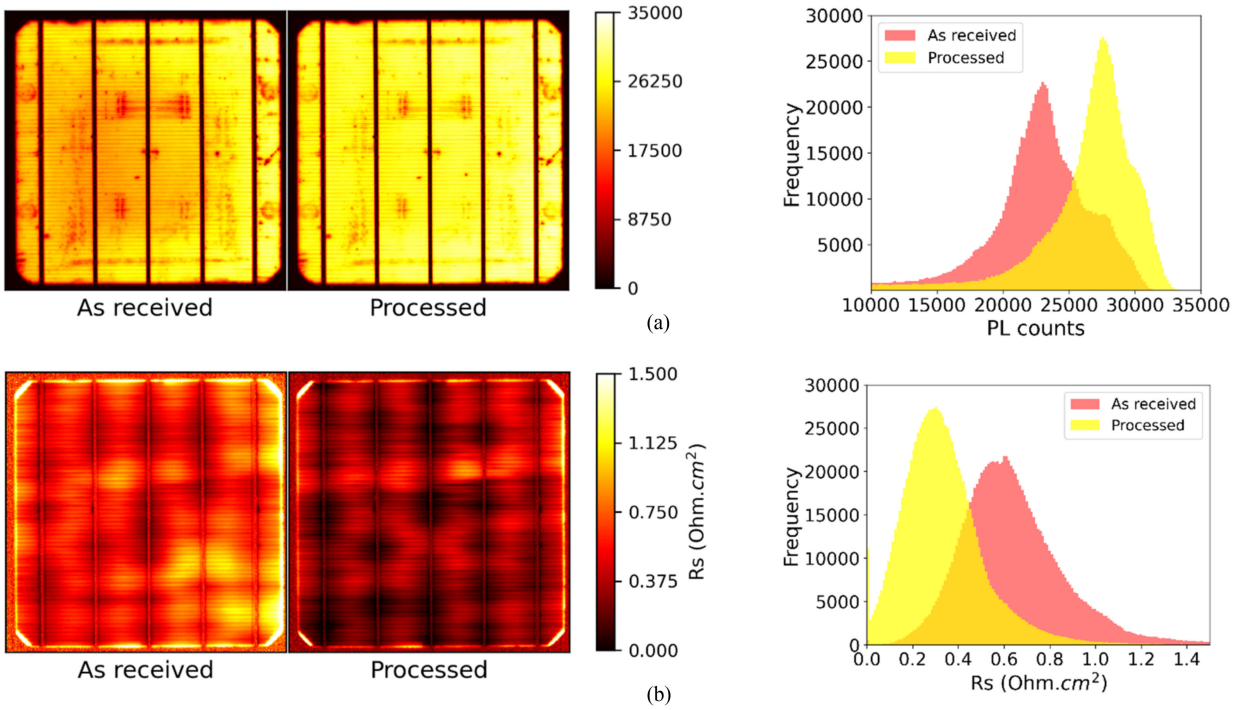

Fig. 3. (a) Open-circuit PL image and (b) series resistance mapping before/after the high intensity illuminated annealing. A frequency histogram, extracted from the displayed image, is also displayed.

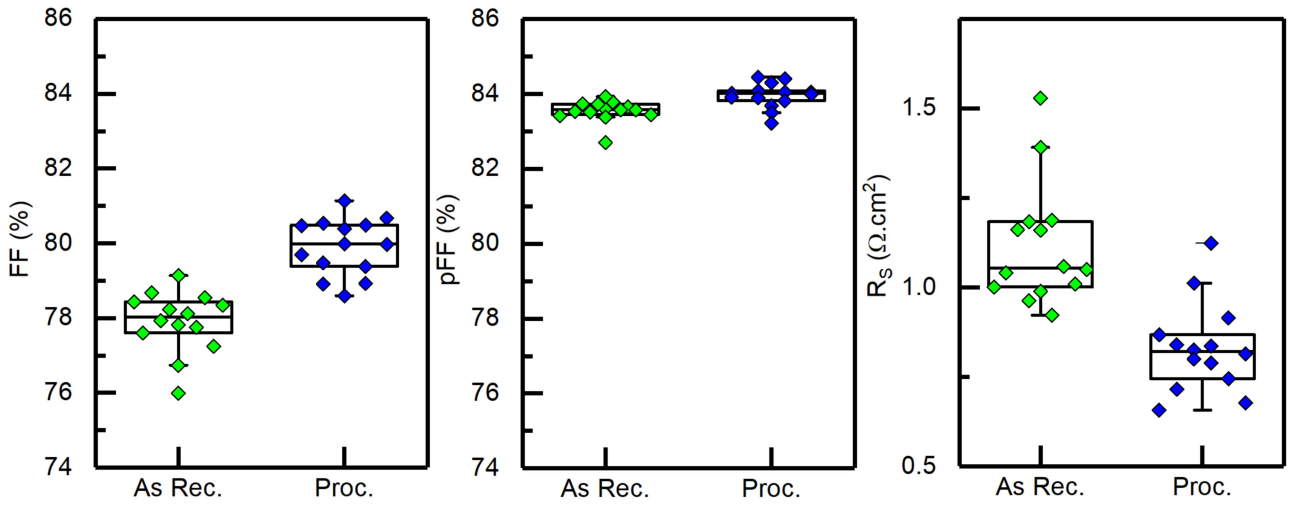

Fig. 4. Box plots displaying changes in FF, pFF, and R_S for cells from company X before/after high intensity illuminated annealing.

a doped a-Si:H layer on top of the intrinsic layer. In this case, light soaking was performed at 25 °C under 1-sun AM 1.5G conditions and the changes in lifetime were observed over hundreds of hours. They showed that, unlike bulk a-Si:H solar cells, the photostability of the a-Si:H/c-Si interface is largely governed by the initial density of interfacial defects, rather than changes in the microstructure in the a-Si:H layer. As such, they attribute the larger improvements in stacks containing doped a-Si:H layers to the higher interfacial defect concentration, due to the presence of the doped layer and a reduced generation of defects due to the field effect provided by the doped layer. This increase in lifetime was extended by Kobayashi *et al.*, [27] who showed an increase in V_{OC} on n-type SHJ solar cells after extended light soaking at 1 sun conditions. This led to an efficiency enhancement of $0.3\%_{abs}$, which saturated after ∼15 h. This increase was also related to a reduction in the density of interfacial defect states. Multiple reports have also indicated that annealing at temperature higher than 200 °C can lead to performance reductions [37], [38]. One key difference between these prior studies and the work reported herein is the intensity of the illumination during light soaking. It is likely that the previously discussed mechanism of improved surface passivation via hydrogen passivation

of interfacial surface defects is occurring in this study, which corresponds with the increased V_{OC} in Fig. 2. However, the high intensity of the light significantly accelerates this reaction and leads to a larger increase compared to light soaking under 1-sun conditions. As such, this demonstration moves the concept of annealing industrial n-type SHJ cells closer to a commercial application.

While the results displayed in Fig. 2 are very promising, further work is required to understand the photostability of surface passivation in SHJ cells. This is highlighted by Madumelu *et al.* [39] who actually showed substantial efficiency reductions in industrial n-type SHJ cells under light soaking at 160 °C [40]. Dark annealing under the same conditions caused a slight increase in efficiency. They also showed that increasing the light intensity up to 40 kW/ m^2 can alter the kinetics of the subsequent recovery of efficiency. This indicates that the meta stable state achieved at the a-Si:H/c-Si interface is very sensitive to annealing conditions. As shown in Fig. 2, the cells from Company Y responded differently to the others. The efficiency enhancement was much smaller. Additionally, unlike the other groups for which the J_{SC} was very stable, the J_{SC} for cells from Company Y underwent a reduction. All of the results in Fig. 2 used a set point temperature of 200 °C (sample temperature of ∼255 °C). When samples from Company Y were subjected to illuminated annealing at higher set point temperatures (data not shown), the reduction in J_{SC} was exacerbated. It is currently not clear what caused this loss in J_{SC}. It may be related to variations in the type of doped interlayers used; however, this information is not available. A recent report by Cattin *et al.* [41] provides some insight. They showed that for optimized n-type SHJ cells, light soaking or current injection can cause an efficiency gain of $0.3\%_{\mathrm{abs}}$ over a time frame of ∼100 h. However, light exposure on a non-optimized p-doped layer can have a negative impact on cell efficiency. The observed reduction in V_{OC} and FF is caused by reduced selectivity, which is attributed to defect generation in the p-doped layer (or the a-Si:H(i) layer underneath) via UV light. This provides strong justification for the "rear emitter" design approach for n-type SHJ cells, where the problematic p-doped layer is on the rear of the cell. In light of this literature, the promising results outlined in this article require further consideration before a commercial solution is fully developed.

IV. Conclusion

In this work, we demonstrated the effectiveness of a 30 s high-intensity illuminated annealing process to improve the performance of n-type SHJ solar cells. The intensity of the illumination from the laser was on the order of 100 suns. The initial study was performed on 100 cells fabricated at Hevel LLC. Efficiency enhancements of $0.63\%_{\mathrm{abs}}$ and $0.58\%_{\mathrm{abs}}$ were shown, for cell groups with efficiencies starting at 21.25% and 22.53%, respectively. This improvement is attributed to increased V_{OC} and FF. The wide applicability of this approach was then demonstrated by testing on cells from five different SHJ cell manufacturers. Efficiency enhancements seen on this range of industrial n-type cells varied from $0.37\%_{\mathrm{abs}}$ to $0.70\%_{\mathrm{abs}}$, indicating the widely applicable nature of this annealing approach. This indicates that not only can the high-intensity illumination significantly accelerate the cell improvement compared to 1-sun, from >10 h to a matter of seconds; the achievable efficiency boost is also larger. Future work will focus on studying the kinetics of this illuminated annealing process to identify a minimum processing time, such that this improvement can be achieved in a commercial manufacturing environment.

Acknowledgment

The views expressed herein are not necessarily the views of the Australian Government, and the Australian Government does not accept responsibility for any information or advice contained herein. The authors would like to thank the various industrial silicon heterojunction solar cell manufacturers for providing cells for use in this work and also would like to thank B. Vicari Stefani for useful scientific discussions. They also acknowledge the kind assistance of staff at the UNSW Solar Industrial Research Facility (SIRF).

References

[1] K. Yoshikawa *et al.*, "Silicon heterojunction solar cell with interdigitated back contacts for a photoconversion efficiency over 26%," *Nature Energy*, vol. 2, no. 5, 2017, Art. no. 17032.
[2] K. Masuko *et al.*, "Achievement of more than 25% conversion efficiency with crystalline silicon heterojunction solar cell," *IEEE J. Photovolt.*, vol. 4, no. 6, pp. 1433–1435, Nov. 2014.
[3] R. V. K. Chavali, S. De Wolf, and M. A. Alam, "Device physics underlying silicon heterojunction and passivating-contact solar cells: A topical review," *Prog. Photovolt. Res. Appl.*, vol. 26, no. 4, pp. 241–260, 2018.
[4] S. De Wolf, A. Descoeudres, Z. C. Holman, and C. Ballif, "High-efficiency silicon heterojunction solar cells: A review," *Green*, vol. 2, pp. 7–24, 2012.
[5] A. S. Abramov, D. A. Andronikov, S. N. Abolmasov, and E. I. Terukov, "Silicon heterojunction technology: A key to high efficiency solar cells at low cost," in *High-Efficient Low-Cost Photovoltaics: Recent Developments*, V. Petrova-Koch, R. Hezel, and A. Goetzberger, Eds. Cham, Switzerland: Springer, 2020, pp. 113–132.
[6] J. Haschke *et al.*, "The impact of silicon solar cell architecture and cell interconnection on energy yield in hot & sunny climates," *Energy Environ. Sci.*, vol. 10, no. 5, pp. 1196–1206, 2017.
[7] J. Werner, B. Niesen, and C. Ballif, "Perovskite/Silicon tandem solar cells: Marriage of convenience or true love story? – An overview," *Adv. Mater. Interfaces*, vol. 5, no. 1, 2018, Art. no. 1700731.
[8] K. A. Bush *et al.*, "23.6%-Efficient monolithic perovskite/silicon tandem solar cells with improved stability," *Nature Energy*, vol. 2, no. 4, 2017, Art. no. 17009.
[9] Z. Yu, M. Leilaeioun, and Z. Holman, "Selecting tandem partners for silicon solar cells," *Nature Energy*, vol. 1, 2016, Art. no. 16137.
[10] A. Blakers, "Development of the PERC solar cell," *IEEE J. Photovolt.*, vol. 9, no. 3, pp. 629–635, May 2019.
[11] M. A. Green, "The passivated emitter and rear cell (PERC): From conception to mass production," *Sol. Energy Mater. Sol. Cells*, vol. 143, pp. 190–197, 2015.
[12] C. Sen *et al.*, "Eliminating light- and elevated temperature-induced degradation in P-type PERC solar cells by a two-step thermal process," *Sol. Energy Mater. Sol. Cells*, vol. 209, 2020, Art. no. 110470.
[13] A. W. Blakers, A. Wang, A. M. Milne, J. Zhao, and M. A. Green, "22.8% efficient silicon solar cell," *Appl. Phys. Lett.*, vol. 55, no. 13, pp. 1363–1365, 1989.
[14] F. Feldmann, M. Bivour, C. Reichel, M. Hermle, and S. W. Glunz, "Passivated rear contacts for high-efficiency n-type si solar cells providing high interface passivation quality and excellent transport characteristics," *Sol. Energy Mater. Sol. Cells*, vol. 120, pp. 270–274, 2014.
[15] Y. Li, H.-S. Kim, J. Yi, D. Kim, and J.-Y. Huh, "Improved electrical performance of low-temperature-cured silver electrode for silicon heterojunction solar cells," *IEEE J. Photovolt.*, vol. 8, no. 4, pp. 969–975, Jul. 2018.
[16] S. De Wolf and M. Kondo, "Nature of doped a-Si:H/c-Si interface recombination," *J. Appl. Phys.*, vol. 105, no. 10, 2009, Art. no. 103707.

[17] B. Hallam *et al.*, "The role of hydrogenation and gettering in enhancing the efficiency of next-generation si solar cells: An industrial perspective," *Phys. Status Solidi Appl. Mater. Sci.*, vol. 214, no. 7, 2017, Art. no. 1700305.
[18] S. De Wolf and M. Kondo, "Boron-doped a-Si:H/c-Si interface passivation: Degradation mechanism," *Appl. Phys. Lett.*, vol. 91, no. 11, 2007, Art. no. 112109.
[19] H. Fischer and W. Pschunder, "Investigation of photon and thermal induced changes in silicon solar cells," in *Proc. 10th IEEE Photovolt. Specialists Conf.*, 1973, pp. 404–411.
[20] K. Bothe and J. Schmidt, "Electronically activated boron-oxygen-related recombination centers in crystalline silicon," *J. Appl. Phys.*, vol. 99, no. 1, 2006, Art. no. 13701.
[21] J. Lindroos and H. Savin, "Review of light-induced degradation in crystalline silicon solar cells," *Sol. Energy Mater. Sol. Cells*, vol. 147, pp. 115–126, 2016.
[22] F. Kersten *et al.*, "Degradation of multicrystalline silicon solar cells and modules after illumination at elevated temperature," *Sol. Energy Mater. Sol. Cells*, vol. 142, pp. 83–86, 2015.
[23] A. C. Wenham *et al.*, "Hydrogen-induced degradation," in *Proc. IEEE 7th World Conf. Photovolt. Energy Convers.*, 2018, pp. 1–8, doi: 10.1109/PVSC.2018.8548100.
[24] D. Chen *et al.*, "Progress in the understanding of light- and elevated temperature-induced degradation in silicon solar cells: A review," *Prog. Photovolt. Res. Appl.*, vol. 29, pp. 1180–1201, 2021.
[25] S. Bao *et al.*, "The rapidly reversible processes of activation and deactivation in amorphous silicon heterojunction solar cell under extensive light soaking," *J. Mater. Sci. Mater. Electron.*, vol. 32, pp. 4045–4052, 2021, doi: 10.1007/s10854-020-05146-0.
[26] M. Wright *et al.*, "Multifunctional process to improve surface passivation and carrier transport in industrial n-type silicon heterojunction solar cells by 0.7% absolute," in *Proc. AIP Conf.*, 2019, Art. no. 110006.
[27] E. Kobayashi *et al.*, "Light-induced performance increase of silicon heterojunction solar cells," *Appl. Phys. Lett.*, vol. 109, no. 15, 2016, Art. no. 153503.
[28] P. Mahtani *et al.*, "Light induced changes in the amorphous—Crystalline silicon heterointerface," *J. Appl. Phys.*, vol. 114, no. 12, 2013, Art. no. 124503.
[29] E. Kobayashi *et al.*, "Increasing the efficiency of silicon heterojunction solar cells and modules by light soaking," *Sol. Energy Mater. Sol. Cells*, vol. 173, pp. 43–49, 2017.
[30] P. Hamer *et al.*, "Investigations on accelerated processes for the boron–oxygen defect in p-type czochralski silicon," *Sol. Energy Mater. Sol. Cells*, vol. 145, pp. 440–446, 2016.
[31] D. N. R. Payne *et al.*, "Acceleration and mitigation of carrier-induced degradation in p-type multi-crystalline silicon," *Phys. Status Solidi – Rapid Res. Lett.*, vol. 10, no. 3, pp. 237–241, 2016.
[32] T. Trupke, R. A. Bardos, M. C. Schubert, and W. Warta, "Photoluminescence imaging of silicon wafers," *Appl. Phys. Lett.*, vol. 89, no. 4, 2006, Art. no. 44107.
[33] H. Kampwerth, T. Trupke, J. W. Weber, and Y. Augarten, "Advanced luminescence based effective series resistance imaging of silicon solar cells," *Appl. Phys. Lett.*, vol. 93, no. 20, 2008, Art. no. 202102.
[34] X. Ru *et al.*, "25.11% efficiency silicon heterojunction solar cell with low deposition rate intrinsic amorphous silicon buffer layers," *Sol. Energy Mater. Sol. Cells*, vol. 215, 2020, Art. no. 110643.
[35] V. Giglia, R. Varache, J. Veirman, and E. Fourmond, "Understanding of the influence of localized surface defectivity properties on the performances of silicon heterojunction cells," *Prog. Photovolt. Res. Appl.*, vol. 28, no. 12, pp. 1333–1344, 2020.
[36] S. De Wolf, S. Olibet, and C. Ballif, "Stretched-exponential a-Si:H/c-Si interface recombination decay," *Appl. Phys. Lett.*, vol. 93, no. 3, 2008, Art. no. 32101.
[37] J.-W. A. Schüttauf *et al.*, "High quality crystalline silicon surface passivation by combined intrinsic and n-type hydrogenated amorphous silicon," *Appl. Phys. Lett.*, vol. 99, no. 20, 2011, Art. no. 203503.
[38] J. Haschke *et al.*, "Annealing of silicon heterojunction solar cells: Interplay of solar cell and indium tin oxide properties," *IEEE J. Photovolt.*, vol. 9, no. 5, pp. 1202–1207, Sep. 2019.
[39] C. Madumelu *et al.*, "Investigation of light-induced degradation in N-Type silicon heterojunction solar cells during illuminated annealing at elevated temperatures," *Sol. Energy Mater. Sol. Cells*, vol. 218, 2020, Art. no. 110752.
[40] B. Wright, C. Madumelu, A. Soeriyadi, M. Wright, and B. Hallam, "Evidence for a light-induced degradation mechanism at elevated temperatures in commercial n-type silicon heterojunction solar cells," *Sol. RRL*, vol. 4, no. 11, 2020, Art. no. 2000214.
[41] J. Cattin *et al.*, "Influence of light soaking on silicon heterojunction solar cells with various architectures," *IEEE J. Photovolt.*, vol. 11, no. 3, pp. 575–583, May 2021.